

# A highly sensitive SnO<sub>2</sub>–CuO multilayered sensor structure for detection of H<sub>2</sub>S gas

Manish Kumar Verma, Vinay Gupta\*

Electronic Material and Devices Laboratory, Department of Physics and Astrophysics, University of Delhi, Delhi 110007, India

## ARTICLE INFO

### Article history:

Received 24 November 2011  
Received in revised form 23 February 2012  
Accepted 24 February 2012  
Available online 3 March 2012

### Keywords:

SnO<sub>2</sub>–CuO multilayer  
H<sub>2</sub>S sensor  
Thin film  
Pulsed laser deposition

## ABSTRACT

Sensing response characteristics of bare SnO<sub>2</sub> thin film and SnO<sub>2</sub>–CuO multilayered structures having different CuO content (3 vol%, 6 vol% and 12 vol%) towards 20 ppm H<sub>2</sub>S gas has been studied. SnO<sub>2</sub>–CuO multilayered structure having an optimum amount of 3 vol% CuO is found to exhibit a high response of  $2.7 \times 10^4$  at a relatively low operating temperature of 140 °C, with a fast response time ( $t_{90}$ ) of 2 s. The enhanced sensing response and the fast response speed are due to the porous microstructure of the deposited thin films in the multilayered sensor structures and the spill-over of the dissociated H<sub>2</sub>S gas molecules by the CuO layers on the surface of sensing SnO<sub>2</sub> layers.

© 2012 Elsevier B.V. All rights reserved.

## 1. Introduction

Hydrogen sulfide (H<sub>2</sub>S) is a toxic gas with an offensive odour and can cause dizziness, nausea, vomiting, irritation of the eyes and respiratory tract and in extreme cases even dangerous to human life. Recently there have been a few major accidents due to leakage of H<sub>2</sub>S gas leading to numerous human casualties. Therefore detection of H<sub>2</sub>S is of immense importance in the areas of oil and natural gas exploration, hygiene control in the field of dentistry, pharmaceutical industries and automatic ventilation unit. Semiconducting SnO<sub>2</sub> is the most widely used gas sensing elements where suitable metal or metal oxide additives are exploited for improving the response characteristics along with selectivity for a particular gas [1–3]. Enhanced sensing response characteristics for H<sub>2</sub>S gas have been reported for SnO<sub>2</sub> thin film based sensors using various catalysts including CuO, Ag, Fe, etc. [3–6]. Amongst them, CuO is identified to be the most promising for detecting H<sub>2</sub>S gas efficiently [5–8]. In general, the operating temperature of the sensor structures is found to be high, though few reports exist where high response ( $S > 10^3$ ) is reported for low concentration of H<sub>2</sub>S, but poor response speed (2–175 min) is the limitation [7,8].

The results obtained by various workers on SnO<sub>2</sub>–CuO composite structures towards detection of H<sub>2</sub>S gas are summarised in Table 1. High sensing response at low operating temperatures along with fast response speed are the most desirable characteristics for

the fabrication of an efficient gas sensor. The growth kinetics of the sensing film and the nature of dispersal and quantity of the catalyst are reported to influence the response characteristics for H<sub>2</sub>S gas sensor to a great extent [6–15]. There are reports where CuO catalyst is dispersed either in the form of islands or as continuous layer on the surface of SnO<sub>2</sub> film prepared by sputtering and an improvement in the operating temperature has been reported with reasonably high sensor response towards H<sub>2</sub>S gas [15,21]. Few reports are available where bi-layer structures of SnO<sub>2</sub>–CuO have been prepared for gas sensing applications by evaporation and PECVD technique, however, either the operating temperature is too high or the response is low for higher gas concentrations [12,20]. Efforts have also been made towards the preparation of sensor structures after incorporating CuO in the bulk of SnO<sub>2</sub>, but the enhancement in response was not promising [8,16,20,23]. However, to the best of our knowledge, no efforts have been made towards the preparation of multilayered structures of porous SnO<sub>2</sub> thin film with the catalytic layers for detection of H<sub>2</sub>S gas besides the fact that change in the sensor resistance with the interaction of target gas involve the contribution from the entire thickness of the sensing element.

Since gas sensing is a surface phenomenon, the porous microstructure of the sensing element is expected to yield better response characteristics as the target gas molecules diffuse deeper in bulk of the sensing film and interact with large area. The presence of porosity in the sensing layer depends mainly on the growth kinetics. The efficient response characteristics of the sensor depends on the optimization of processing conditions for obtaining porous sensing layer besides the novel design structure. Therefore, the dispersal of CuO catalyst in the interior of the porous

\* Corresponding author. Tel.: +91 9811563101.

E-mail addresses: [vgupta@physics.du.ac.in](mailto:vgupta@physics.du.ac.in), [drvin.gupta@rediffmail.com](mailto:drvin.gupta@rediffmail.com) (V. Gupta).

**Table 1**  
Some important reports on SnO<sub>2</sub>–CuO based sensors for H<sub>2</sub>S gas.

Sensing material	Technique used	Gas conc. (ppm)	Response	Response time (s)	Recovery time (s)	Operating temp (°C)	Ref.
CuO–SnO <sub>2</sub>	Pulsed laser deposition	20	$2.3 \times 10^3$	–	–	100	[6]
CuO–SnO <sub>2</sub> nanowires	Chemical route	20	809	~2	~300	300	[5]
SnO <sub>2</sub> –CuO nanowires	Furnace + drop casting	50	$6 \times 10^6$	–	–	150	[9]
Cu–SnO <sub>2</sub>	Electrostatic sprayed	10	$2.5 \times 10^3$	–	–	100	[10]
CuO–SnO <sub>2</sub>	Screen printing	1	$8 \times 10^3$	15	–	50	[11]
Cu/Sn double layer	Thermal evaporation	3	33	–	–	200	[12]
CuO modified SnO <sub>2</sub> nanoribbons	Oxidation	3	180	15	–	RT	[13]
SnO <sub>2</sub> –ZnO–CuO thick films	Screen printing and firing	50	$6 \times 10^4$	15	7–8 min	250	[14]
CuO islands on SnO <sub>2</sub>	Reactive sputtering	20	$7.4 \times 10^3$	15	118	150	[15]
SnO <sub>2</sub> –CuO composite	Thermal evaporation	50	$2.5 \times 10^4$	80	100	200	[8]
Cu–SnO <sub>2</sub>	Co precipitation	200	~900	$8(t_{63})$	$2(t_{63})$	77	[16]
Cu-doped SnO <sub>2</sub>	Spray pyrolysis	1000	910	10	25 min	200	[17]
CuO–SnO <sub>2</sub>	Thermal evaporation	50	$3.6 \times 10^5$	10 min( $t_{80}$ )	3 min( $t_{80}$ )	160	[18]
CuO-doped SnO <sub>2</sub>	Thermal evaporation	10	~ $10^6$	2 min( $t_{80}$ )	30 min	200	[7]
Cu nanocluster functionalized SnO <sub>2</sub> film	Spray pyrolysis	400	200	60	6 h	RT	[19]
SnO <sub>2</sub> –CuO–SnO <sub>2</sub> composite film	PECVD	50	210	45	41	90	[20]
SnO <sub>2</sub> –CuO	Magnetron sputtering	100	$1.6 \times 10^4$	1 min( $t_{70}$ )	–	170	[21]
SnO <sub>2</sub> –CuO	Low pressure evaporation	10	~ $4 \times 10^2$	–	–	200	[22]
SnO <sub>2</sub> –CuO	Spray pyrolysis	100	$10^4$	14 min	–	150–160	[23]

SnO<sub>2</sub> sensing film in a suitable manner is expected to deplete the entire thickness of sensing layer and helps in getting the enhanced response.

Pulsed laser deposition (PLD) is well known growth technique to produce high quality metal oxide thin film where the porosity can be easily controlled along with in situ dispersal of catalyst in the sensing layer. Recently, it was identified that PLD grown SnO<sub>2</sub> thin films owing to their favourable morphology gives better response for H<sub>2</sub>S gas compared to the one deposited using rf sputtering technique [6]. However, to the best of our knowledge, no report is available on the development of multilayered sensor structures of porous SnO<sub>2</sub> with the catalysts for detection of H<sub>2</sub>S gas.

In the present work an effort has been made to prepare a porous SnO<sub>2</sub>–CuO multilayered sensor structures using PLD technique. The thickness of CuO catalytic layers in the multilayered structure is optimized for the enhanced response characteristics towards H<sub>2</sub>S gas. The proposed multilayered structure is expected to yield better response characteristics due to excellent electronic and chemical interaction of SnO<sub>2</sub> with CuO catalyst under interaction with H<sub>2</sub>S gas molecules.

## 2. Experimental

The thin film of SnO<sub>2</sub> and SnO<sub>2</sub>–CuO multilayer structures have been deposited on the corning glass substrate using PLD technique. The Inter digital electrodes (IDEs) of Platinum (Pt) were patterned on the corning glass substrate using conventional photolithographic technique prior to the deposition of sensing films. The Pt layer of 90 nm thickness was deposited by rf sputtering technique in Argon ambient and a buffer layer of Ti (20 nm) was grown prior to Pt for improvement in the adhesion on corning glass substrate. For the deposition of SnO<sub>2</sub> thin film and SnO<sub>2</sub>–CuO multilayered structures, ceramic pellets of SnO<sub>2</sub> and CuO were prepared by pressing the high purity powders (99.99% pure) using a dye (2.5 cm diameter) by applying a pressure of 110 MPa. The SnO<sub>2</sub> and CuO pellets were sintered at 1350 and 400 °C, respectively for 4 h in a temperature controlled furnace. Thin film of SnO<sub>2</sub> and SnO<sub>2</sub>–CuO multilayer structures were prepared using PLD technique onto IDE/glass substrate at an oxygen pressure of 100 mT without any substrate heating. The fourth harmonic of Nd:YAG laser ( $\lambda = 266$  nm) at a pulse rate of 5 Hz and fluence of  $1.2 \text{ J cm}^{-2}$  was used to ablate the ceramic targets. A schematic of

both the sensor structures prepared in the present work is shown in Fig. 1. The total thickness of all prepared sensors (bare SnO<sub>2</sub> thin film and SnO<sub>2</sub>–CuO multilayered structure) was fixed at 90 nm. SnO<sub>2</sub>–CuO multilayered sensor structure was fabricated by ablating the SnO<sub>2</sub> and CuO targets sequentially. Ten layers of each material was deposited by varying number of laser pulses for the respective targets while maintaining the total number of laser shots fixed at 3300. The multilayered (SnO<sub>2</sub>–CuO) sensor structures having CuO content of 3 vol%, 6 vol% and 12 vol% were obtained respectively by using 320, 310, and 290 shots for SnO<sub>2</sub> for each layer while 10, 20, and 40 shots for each layer of CuO. The percentage doping of CuO (in volume percentage) in the multilayered (SnO<sub>2</sub>/CuO/SnO<sub>2</sub>/.../CuO) sensor structure was calculated from the thickness of the individual SnO<sub>2</sub> and CuO thin films after calibration with respect to the number of shots of laser pulses. Thin films of both SnO<sub>2</sub> and CuO were deposited separately using 300 laser shots under optimized processing conditions and their thickness were measured using surface profiler. The thickness of each layer (SnO<sub>2</sub> or CuO) in the multilayered structure was obtained from the number of shots of the laser pulses used for respective target, and subsequently the volume percentage of the CuO in multilayered sensor structure was determined. The bare SnO<sub>2</sub> thin film sensor is labelled as C0, whereas SnO<sub>2</sub>–CuO multilayered sensor structures having 3 vol%, 6 vol% and 12 vol% CuO content were labelled as C1, CII and CIII, respectively. All the prepared sensor structures (C0, C1, CII and CIII) were annealed in air at 300 °C for 2 h to stabilize the sensor resistance [6]. The crystallographic structure of prepared thin films was studied using X-ray diffractometer (Bruker D8-Discover, Germany) using Cu K $\alpha$ 1 source. Optical properties of the sensing layer were investigated using UV–visible spectrophotometer (PerkinElmer lambda 35, USA). The microstructure of the sensor surface was studied using atomic force microscopy (AFM, Veeco DCP2, USA). The thickness of thin films was measured using surface profilometer (Dektak 150, VEECO, USA). The sensing response characteristics of the prepared sensors were obtained in a special design test gas chamber over a wide temperature range (80–260 °C). The sensor resistance was measured using a digital multimeter (Keithley 2002) interfaced with a PC for data acquisition. At a specific temperature, the sensor was first stabilized under clean dry air. After attaining a stable resistance ( $R_a$ ) the test chamber was first evacuated and subsequently synthetic dry air mixed with required concentration of target gas (H<sub>2</sub>S) was made to flow using calibrated leaks through needle valves, till the test chamber acquired the atmospheric pressure. During recovery study, the target gas

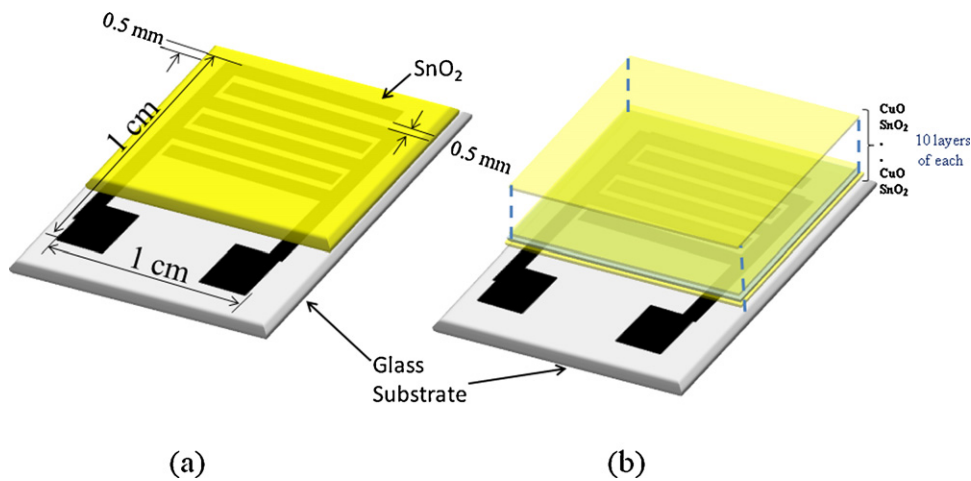


Fig. 1. Schematic of the prepared sensor structures (a) pure SnO<sub>2</sub> film and (b) SnO<sub>2</sub>–CuO multilayered structure.

was flushed out of the test chamber by creating vacuum again and clean dry air was introduced. The sensing response of a sensor for reducing gas is defined as  $S = R_a/R_g$ , where  $R_a$  is the sensor resistance in clean dry air, and  $R_g$  is the sensor resistance measured in the presence of reducing gas (H<sub>2</sub>S).

### 3. Results and discussion

The as-deposited SnO<sub>2</sub> thin films were found to be transparent and strongly adherent to the substrate. From the XRD analysis, it is noted that the as-deposited SnO<sub>2</sub> thin films were amorphous and becomes polycrystalline after post-deposition annealing treatment in air at 300 °C for 2 h. Fig. 2 shows the XRD pattern of all the prepared sensor structures (C0, C1, CII and CIII) subject to a post deposition annealing treatment. Broad and well defined XRD peaks were observed for sample C0 at  $2\theta = 26.5^\circ$ ,  $33.9^\circ$ ,  $38.1^\circ$  and  $51.8^\circ$  (Fig. 2) corresponding to (1 1 0), (1 0 1), (2 0 0) and (2 1 1) planes of the rutile structure of SnO<sub>2</sub>, respectively [1]. The obtained results confirm the formation of a single phase and polycrystalline SnO<sub>2</sub> thin film after a post-deposition annealing treatment. It is also important to note from Fig. 2 that a small XRD peak starts appearing in the multilayered structures (C1, CII, and CIII) at around  $2\theta = 35.4^\circ$  and was corresponding to the (0 0 2) plane of CuO [5]. The intensity of this XRD peak (0 0 2), starts increasing with increase in CuO

content in the multilayered structure and becomes prominent for sample CIII (12 vol% CuO content). The presence of XRD peaks corresponding to both SnO<sub>2</sub> and CuO confirm the formation of SnO<sub>2</sub>–CuO composite sensor in the form of multilayered structure. The value of crystallite size of sensing SnO<sub>2</sub> film was evaluated using the well known Scherrer formula  $d = K\lambda/\beta \cos \theta$ , where  $K$  is 0.94,  $\lambda$  is X-ray wavelength (1.5406 Å),  $\beta$  is full width at half maxima (FWHM) of (1 0 1) XRD peak, and  $\theta$  is the corresponding diffraction angle. The estimated value of the crystallite size for SnO<sub>2</sub> thin film was around 8 nm. The FWHM of (1 0 1) XRD peak was found to increase in the multilayered sensor structure with increase in the CuO content (Fig. 2). A slight decrease in the grain size is observed from 8 nm to 5 nm for the SnO<sub>2</sub>–CuO multilayered structure having 12 vol% CuO with respect to that of bare SnO<sub>2</sub> thin film.

Fig. 3 shows the UV–visible spectra of the SnO<sub>2</sub> thin film and all prepared multilayered sensor structures. SnO<sub>2</sub> thin film was found to be highly transparent (~80%) in the visible region with the onset of a sharp absorption edge at around 350 nm (Fig. 3). A slight decrease in the transmittance was noted with the increase in CuO content in the multilayered structure. The optical bandgap ( $E_g$ ) of films was evaluated by extrapolating the linear portion of Tauc plot between  $(\alpha h\nu)^2$  versus  $h\nu$  to  $\alpha = 0$ , where  $\alpha$  is the absorption coefficient and  $h\nu$  is the photon energy. Estimated value of the bandgap was around 3.98 eV for the SnO<sub>2</sub> thin film (sample C0) and is in good agreement with the values reported by other workers for SnO<sub>2</sub> thin films [24,25]. The value of bandgap decreases slowly from

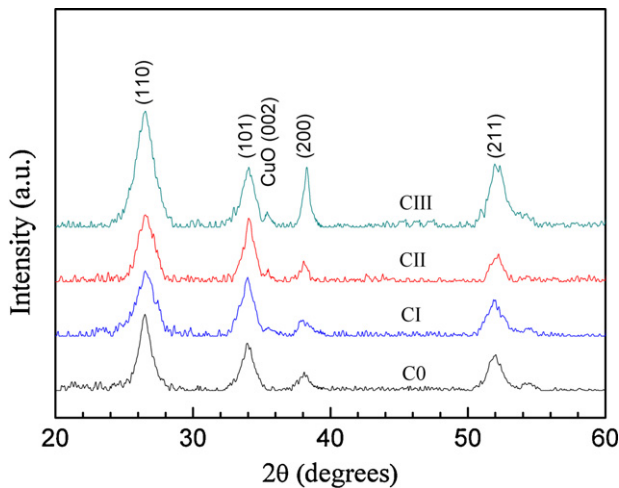


Fig. 2. XRD pattern of the SnO<sub>2</sub> thin film based sensor structures (C0, C1, CII and CIII).

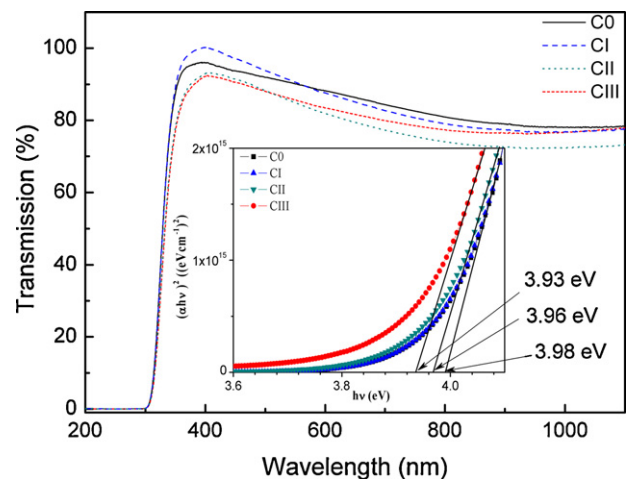


Fig. 3. Transmission spectra of the sensor structures (C0, C1, CII and CIII).

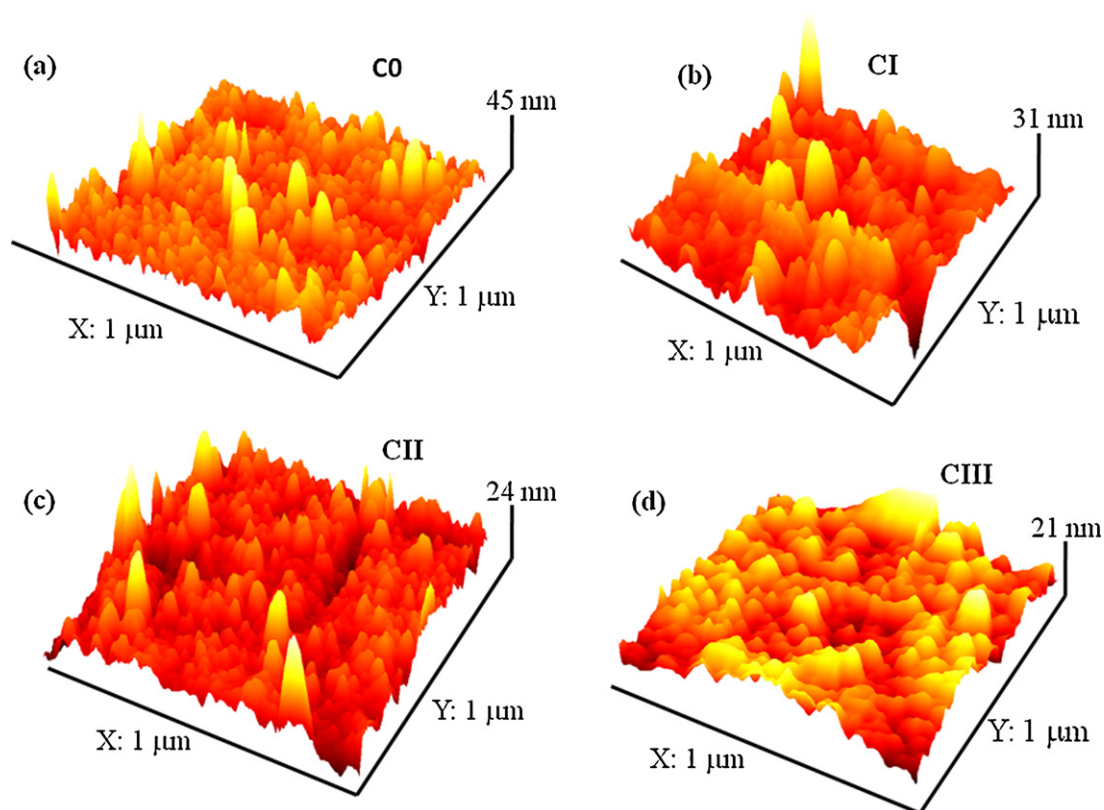


Fig. 4. 3D AFM images of the surface of sensors samples C0, CI, CII and CIII.

3.98 eV to 3.93 eV with the increase in CuO content in the SnO<sub>2</sub>–CuO multilayered structure from 3 vol% to 12 vol% (inset of Fig. 3). The lower value of band gap obtained for the SnO<sub>2</sub>–CuO multilayered structure is attributed to the fact that CuO has relatively lower value of bandgap (1.2–1.9 eV) in comparison to that of SnO<sub>2</sub> (3.6–4.2 eV) [24–27].

Fig. 4(a–d) shows the AFM images of the surface of all the prepared sensor structures (C0, CI, CII, and CIII). The surface morphology of all prepared samples was found to be rough and porous. The SnO<sub>2</sub>–CuO multilayered structure (Sample CI) having 3 vol% CuO shows the maximum root mean square roughness (30 nm) and the porosity in comparison to that of other sensor structures (Fig. 4). The 2D AFM images of the surface of samples C0 and CI is shown in Fig. 5. It can be noted from Fig. 5 that the surface morphology of sensor CI (3 vol% CuO) has a higher porosity in comparison to

that observed in sensor C0 (bare SnO<sub>2</sub> film). The porosity and surface roughness is seen to be decreasing with further increase in the content of CuO (>3 vol%) in the multilayered structure (Fig. 4), and may be attributed to the decrease in grain size. The presence of large amount of porosity and high surface roughness for sample CI seems to be advantageous for obtaining the enhanced response due to availability of large area of sensing layer for interaction with the target gas molecules.

### 3.1. Sensing response characteristics

Sensing response characteristics of the bare SnO<sub>2</sub> thin film (Sample C0) and CuO–SnO<sub>2</sub> multilayered structures (Samples CI, CII and CIII) were investigated over a temperature range of 80–260 °C for 20 ppm of H<sub>2</sub>S gas and are shown in Fig. 6. The response of

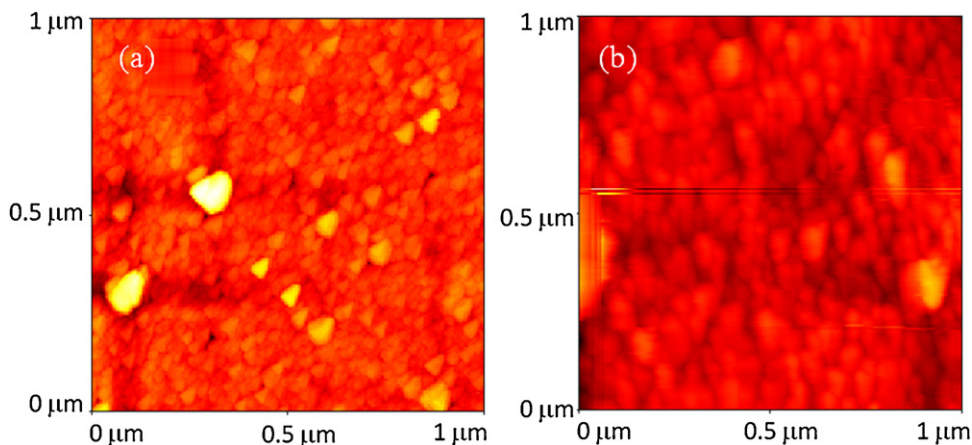


Fig. 5. 2D AFM images of sensors C0 and CI.

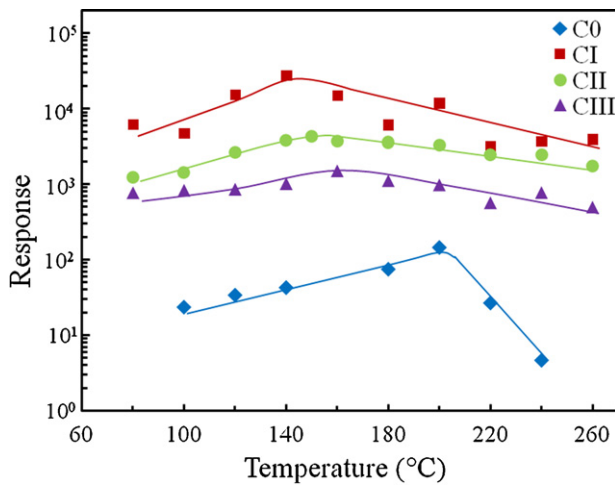


Fig. 6. Variation of response with temperature for sensors C0, C1, C2 and C3 towards 20 ppm H<sub>2</sub>S gas.

all prepared sensors increases initially with increase in temperature, attaining a maximum response at a particular temperature ( $T_{OP}$ ) and thereafter shows a decrease. The maximum response of bare SnO<sub>2</sub> thin film sensor (C0) was about  $1.5 \times 10^2$  at an operating temperature of 200 °C. The sensor response was found to increase by about two orders of magnitude along with a reduction in the operating temperature after integration of CuO thin film with SnO<sub>2</sub> layer in the multilayered sensor structures (Samples C1, C2, and C3) (Fig. 6). The observed results indicate the importance of introduction of catalytic CuO layer in the SnO<sub>2</sub> based H<sub>2</sub>S gas sensors towards both the enhanced response and lower operating temperature. The sensing parameters including sensor response, response time and operating temperature obtained for all prepared sensor structures towards 20 ppm H<sub>2</sub>S gas at their respective operating temperatures are presented in Table 2. The SnO<sub>2</sub>-CuO multilayered structure (Sample C1) having 3 vol% CuO exhibits the maximum sensing response of  $2.7 \times 10^4$  for 20 ppm H<sub>2</sub>S at a relatively much lower operating temperature (140 °C). The sensing response characteristics (high response, low operating temperature and fast response speed) obtained for sample C1 are much superior compared to the corresponding reported results by other workers for composite SnO<sub>2</sub>-CuO structures (Table 1). The observed high response for the prepared multilayered sensor structure is attributed to the distribution of optimum content (3 vol%) of CuO layers within the porous SnO<sub>2</sub> layers thereby resulting in the maximum modulation of space charge region extended throughout the sensing layer with the interaction of target gas (H<sub>2</sub>S). It is interesting to note from Fig. 6 and Table 2 that with further increase in the CuO content in the multilayered structures (Samples C2 and C3), a decrease in the sensor response is observed along with an increase in the operating temperature (150 °C and 160 °C). The observed decrease in the sensor response with increase in CuO content in the multilayered structure can be correlated with the decrease in porosity of the films. As the porosity of the film decreases, less number of H<sub>2</sub>S gas molecules can diffuse into the interior of the sensing layer, therefore, interaction of H<sub>2</sub>S gas

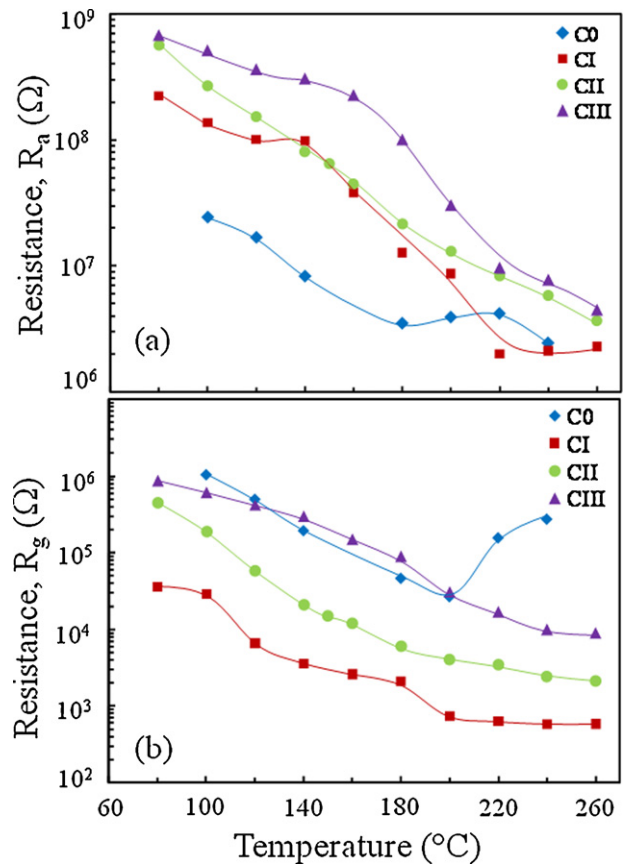


Fig. 7. Variation of (a) resistance ( $R_a$ ) as a function of temperature for the sensors C0, C1, C2 and C3 in air (b) resistance ( $R_g$ ) with temperature for the sensors C0, C1, C2 and C3 in the presence of 20 ppm H<sub>2</sub>S gas.

molecules with sensing element reduces thereby giving lower sensor response (Fig. 6).

Fig. 7(a) shows the variation of sensor resistance measured in atmospheric air ( $R_a$ ) for all the samples (C0, C1, C2 and C3) as a function of temperature. It may be seen that the resistance ( $R_a$ ) of all the sensor structures decreases with an increase in temperature and is in accordance with the semiconducting behaviour of metal oxide (SnO<sub>2</sub> and CuO) thin films. The initial resistance ( $R_a$ ) of the SnO<sub>2</sub> thin film sensor increases by about an order of magnitude (Fig. 7(a)) with the incorporation of CuO layer (multilayered sensor structure). It is well known that CuO is a p-type semiconductor, whereas SnO<sub>2</sub> is an n-type, therefore p-n junctions are formed at the interfaces of CuO-SnO<sub>2</sub> in the multilayered sensor structures. The formation of space charge regions at the CuO-SnO<sub>2</sub> interfaces result in a decrease in the concentration of electrons in the conduction band of SnO<sub>2</sub> thin film thereby giving a higher value of sensor resistance ( $R_a$ ) for the multilayered structures. Also the presence of CuO catalyst leads to an accelerated activity of adsorption of oxygen from atmosphere on the surface of SnO<sub>2</sub> thin films [15]. Therefore the capturing of electrons from the conduction band of SnO<sub>2</sub> by the adsorbed oxygen also increases [15]. The combined effect of these two factors (formation of p-n junctions and adsorbed oxygen)

Table 2

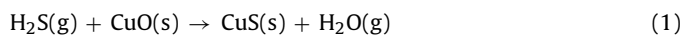
The sensing response parameters obtained for sensors C0, C1, C2, and C3.

Sample	Operating temp. (°C)	$R_a$ ( $\Omega$ )	$R_g$ ( $\Omega$ )	Response time ( $t_{90}$ ) (s)	Response
C0	200	$3.9 \times 10^6$	$2.6 \times 10^4$	4	$1.4 \times 10^2$
C1	140	$9.8 \times 10^7$	$3.6 \times 10^3$	2	$2.7 \times 10^4$
C2	150	$6.5 \times 10^7$	$1.5 \times 10^4$	2	$4.3 \times 10^3$
C3	160	$2.3 \times 10^8$	$1.5 \times 10^5$	3	$1.5 \times 10^3$

results in a higher sensor resistance for the SnO<sub>2</sub>-CuO multilayered structure in comparison to that of bare SnO<sub>2</sub> thin film sensor (Fig. 7(a)). It is important to note from Fig. 7(a) that the sensor resistance ( $R_a$ ) increases continuously with increase in CuO content in the multilayered structures. The observed increase in  $R_a$  is due to increase in the depletion width at the CuO-SnO<sub>2</sub> interfaces along with enhanced oxygen adsorption activity on the sensor surface as more content of CuO catalyst is present in the multilayered sensor structure.

A hump in the variation of sensor resistance ( $R_a$ ) with temperature for C0 sample is observed at around 220 °C (Fig. 7(a)), which is attributed to the enhanced adsorption activity of oxygen and the conversion of adsorbed molecular oxygen (O<sub>2</sub><sup>-</sup>) to atomic oxygen (2O<sup>-</sup>) at elevated temperature [15,28]. For multilayered sensor samples (CI, CII and CIII), the region of enhanced oxygen adsorption is observed in the lower temperature region of 120–180 °C. In the SnO<sub>2</sub>-CuO multilayered sensors, CuO layers are embedded within the SnO<sub>2</sub> layers throughout the porous sensor structure. Therefore a continuous chain of p-n-p-n junctions is formed in the multilayered structure and the entire sensor structure is expected to have the space charge region.

The variation of sensor resistance in the presence of 20 ppm target H<sub>2</sub>S gas ( $R_g$ ) for all prepared sensor structures is shown in Fig. 7(b). It is observed that the sensor resistance ( $R_g$ ) in the presence of H<sub>2</sub>S gas is reduced by about two orders in magnitude as compared to the resistance measured in air ( $R_a$ ) for bare SnO<sub>2</sub> thin film sensor (C0). However, the observed decrease in sensor resistance ( $R_a$  to  $R_g$ ) for multilayered structures (CI, CII and CIII) with the interaction of H<sub>2</sub>S gas was more than three orders in magnitude at their operating temperature (Fig. 7). The fall in sensor resistance ( $R_a$  to  $R_g$  at  $T = T_{OP}$ ) was found to be maximum for sample CI, whereas starts decreasing with increase in CuO content in the multilayered structure (Samples CII and CIII). The observed behaviour is in accordance with our earlier discussion related to the importance of porosity in obtaining the enhanced sensing response due to diffusion of more H<sub>2</sub>S molecules into the interior of the sensing layer and providing large surface area for interaction. The decrease in sensor resistance from  $R_a$  to  $R_g$  is due to the interaction of target gas molecules with the adsorbed oxygen on the surface of SnO<sub>2</sub> layers. The desorbed oxygen releases the trapped electrons and therefore a significant decrease in the sensor resistance from  $R_a$  to  $R_g$  is observed. The availability of large concentration of adsorbed oxygen on SnO<sub>2</sub> surface and the modulation of depletion region at the CuO-SnO<sub>2</sub> interface in the multilayered sensor structures (CI, CII and CIII) are expected to result in much higher decrease in the sensor resistance from  $R_a$  to  $R_g$  with H<sub>2</sub>S gas interaction. On exposure to the multilayered sensor with reducing target gas H<sub>2</sub>S, the CuO catalyst converts to CuS by the following reaction



CuS is less p-type relative to CuO and therefore the width of the space charge region in the SnO<sub>2</sub> layer (at CuO-SnO<sub>2</sub> interface) is reduced. The reduction in depletion region facilitates the easier flow of electrons through the sensing SnO<sub>2</sub> layer, resulting in a lower value of the sensor resistance with interaction of H<sub>2</sub>S gas. As the percentage of CuO in the multilayered sensor structure increases the porosity starts reducing, which restricts the diffusion of H<sub>2</sub>S molecules deeper inside the sensing film. Therefore, depletion width of the p-n junctions available near the sensor surface are modulating with the interaction of H<sub>2</sub>S gas molecules while those available deeper in the sensor structures are not disrupted. As a result, SnO<sub>2</sub>-CuO multilayered structure having more content of CuO (samples CII and CIII) shows relatively less decrease in resistance from  $R_a$  to  $R_g$  when target H<sub>2</sub>S gas interacts with the sensor surface. The multilayered sensor structure having 3 vol% CuO (Sample CI) shows a maximum response ( $2.7 \times 10^4$ ) amongst all

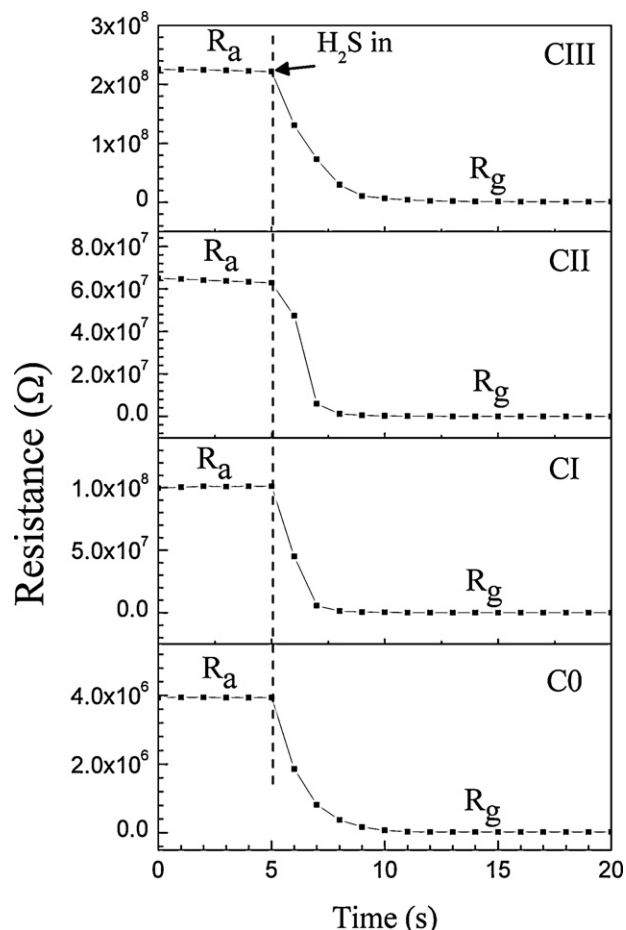
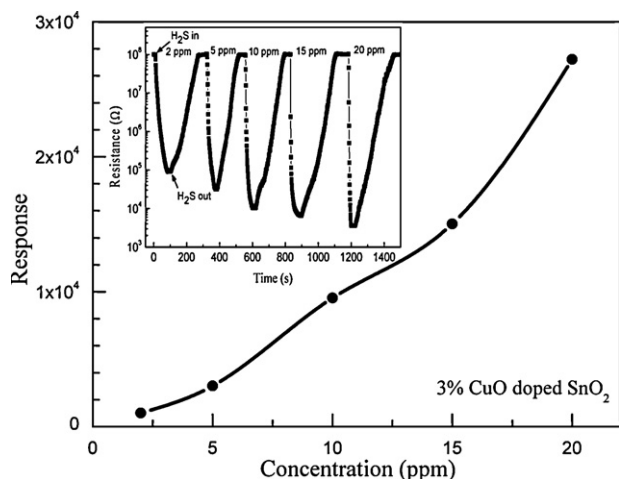


Fig. 8. Variation of resistance of the sensors C0, CI, CII and CIII with time at their respective operating temperature.

the sensor structures at a relatively lower operating temperature of 140 °C. This is due to the porous microstructure of CI sample, resulting in more diffusion of H<sub>2</sub>S gas molecules in the interior of multilayered sensor. The interaction of H<sub>2</sub>S gas results in modulation of the depletion width of the p-n junctions at CuO-SnO<sub>2</sub> interfaces in sample CI to the maximum extent besides the release of trapped electrons in large amount by the oxygen desorbed from sensing SnO<sub>2</sub> layer. It is important to point out that the CuO catalyst is known to spillover the H<sub>2</sub>S gas molecule over the surface of sensing SnO<sub>2</sub> layer [15] and therefore interact effectively in large amount with the adsorbed oxygen molecules in multilayered sensor (Sample CI). It is also interesting to note from Fig. 6 that the sensor CI exhibits a moderate response  $\sim 6.2 \times 10^3$  at even lower operating temperatures (80 °C) with a fast response time of 3 s. Therefore the sample CI could also be utilized at low temperature with efficient response characteristics.

The variation in resistance of four sensor structures (C0, CI, CII and CIII) with the interaction of H<sub>2</sub>S gas (20 ppm) at their operating temperature is shown in Fig. 8 as a function of time. All the sensors achieve 90% of the change in resistance from  $R_a$  to  $R_g$  in a very small time (2–4 s) and subsequently saturate to a minimum value of  $R_g$ . The tailing end of the sensor resistance towards minimum saturation value (Fig. 8) is due to the diffusion of the target gas (H<sub>2</sub>S) molecules into the interior of porous sensing film, which is a slow process. It can be observed from Fig. 8 that the response time ( $t_{90}$ ) for the SnO<sub>2</sub>-CuO multilayered structures are lower in comparison to that of bare SnO<sub>2</sub> thin film sensor. Furthermore, the response time shows a slight increase (2–3 s) with increase in CuO content in the multilayered structure and may be attributed to a



**Fig. 9.** Variation of the response of sensor CI as a function of H<sub>2</sub>S gas concentration. Inset shows the change in sensor resistance with time with the interaction of varying H<sub>2</sub>S gas concentration.

decrease in the porosity of sensing film (Fig. 8). As the porosity of sensing film is decreasing, the target gas molecules are expected to take more time to diffuse in the interior of the sensing layer, thereby resulting in higher response time.

It may be noted that the short term (15 min) and long term (8 h time weighted average) exposure limit for H<sub>2</sub>S gas at the workplace is 5 ppm and 1 ppm respectively as per the report of the American Conference of Governmental Industrial Hygienists (ACGIH) 2010. The optimized multilayer sensor structure fabricated in the present work has been studied for the variation in sensing response with varying concentration of H<sub>2</sub>S gas over the range 2–20 ppm (Fig. 9). The sensing response was found to increase almost linearly from  $1.02 \times 10^3$  to  $2.70 \times 10^4$  with increase in H<sub>2</sub>S gas concentration from 2 ppm to 20 ppm (Fig. 9), indicating the applicability of the prepared sensor structure for the real field application. Inset of Fig. 9 shows the variation of sensor resistance for the sample CI with varying concentration of H<sub>2</sub>S gas from 2 ppm to 20 ppm at its operating temperature (140 °C). The behaviour of change in sensor resistance from  $R_a$  to  $R_g$  was found to be similar over the entire measured range of H<sub>2</sub>S gas concentrations. The sensor regains the initial resistance value ( $R_a$ ) quickly after removal of target H<sub>2</sub>S gas (inset of Fig. 9). It is important to note from Fig. 9, that the sensor CI has

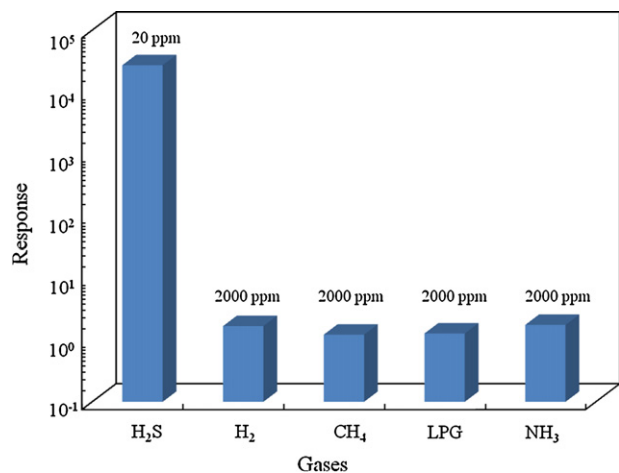


**Fig. 10.** Cross sensitivity study at operating temperature of the sensor CI (140 °C) with H<sub>2</sub>, CH<sub>4</sub>, LPG and NH<sub>3</sub> gases.

the remarkable response ( $1.02 \times 10^3$ ) to a very low concentration (2 ppm) of the H<sub>2</sub>S gas also. Therefore, the SnO<sub>2</sub>–CuO multilayered sensor structure fabricated in the present study with 3 vol% content of CuO catalyst has the potential of detection of H<sub>2</sub>S gas efficiently over a wide concentration range with enhanced response characteristics.

The selectivity study was also carried for multilayered sensor structure having 3 vol% CuO catalyst (Sample CI), towards other interfering gases (H<sub>2</sub>, CH<sub>4</sub>, LPG, NH<sub>3</sub>) and the obtained response for different gases is shown in Fig. 10. The concentration of all interfering gases is kept higher (2000 ppm), while the concentration of H<sub>2</sub>S gas is fixed at 20 ppm. It may be seen from Fig. 10 that the multilayered sensor (CI) is highly selective towards the H<sub>2</sub>S gas only, while other interfering gases give negligible response ( $\sim 1$ ) even for their high concentrations.

#### 4. Conclusion

The SnO<sub>2</sub>–CuO multilayered sensor with 3 vol% CuO content exhibits enhanced response characteristics for H<sub>2</sub>S gas over the concentration range from 2 ppm to 20 ppm. The sensing response of bare SnO<sub>2</sub> thin film sensor was  $1.4 \times 10^2$  with a response time of 4 s at an operating temperature of 200 °C. The integration of CuO layers with SnO<sub>2</sub> thin films results into enhanced response by two orders in magnitude. Maximum response of  $2.7 \times 10^4$  towards 20 ppm H<sub>2</sub>S was achieved for multilayered sensor structure having 3 vol% CuO with a relatively fast response time of 2 s. The observed enhanced response characteristics towards H<sub>2</sub>S gas is attributed to the twin effect of the modulation of depletion width at the p–n junctions of CuO–SnO<sub>2</sub> interfaces and the accelerated oxygen adsorption activity on SnO<sub>2</sub> film due to the presence of CuO catalyst in the multilayered sensor structure. Porosity of the films is important that allows the diffusion of large concentration of target gas molecules into the interior of multilayered sensor structure and thus providing enhanced interaction of sensing layer with the target gas molecules.

#### Acknowledgements

The authors acknowledge the financial support provided by the Department of Science and Technology (DST), National Programme for Micro and Smart Systems (NPMAS) and Department of Information Technology (DIT), Government of India. One of the authors (M K V) is thankful to CSIR for research fellowship.

#### References

- [1] K. Ihokura, J. Watson, The Stannic Oxide Gas Sensor, Principles and Applications, CRC Press, Boca Raton, FL, 1994.
- [2] A. Sharma, M. Tomar, V. Gupta, Low temperature operating SnO<sub>2</sub> thin film sensor loaded with WO<sub>3</sub> micro-discs with enhanced response for NO<sub>2</sub> gas, Sens. Actuators B 161 (2012) 1114–1118.
- [3] J. Gong, Q. Chen, M.R. Lian, N.C. Liu, R.G. Stevenson, F. Adami, Micromachined nanocrystalline silver doped SnO<sub>2</sub> H<sub>2</sub>S sensor, Sens. Actuators B 114 (2006) 32–39.
- [4] M.V. Vaishampayan, R.G. Deshmukh, P. Walke, I.S. Mulla, Fe-doped SnO<sub>2</sub> nano-material: a low temperature hydrogen sulphide gas sensor, Mater. Chem. Phys. 109 (2008) 230–234.
- [5] I.S. Hwang, J.K. Choi, S.J. Kim, K.Y. Dong, J.H. Kwon, B.K. Ju, J.H. Lee, Enhanced H<sub>2</sub>S sensing characteristics of SnO<sub>2</sub> nanowires functionalized with CuO, Sens. Actuators B 142 (2009) 105–110.
- [6] M. Verma, A. Chowdhuri, K. Sreenivas, V. Gupta, Comparison of H<sub>2</sub>S sensing response of hetero-structure sensor (CuO–SnO<sub>2</sub>) prepared by rf and pulsed laser deposition, Thin Solid Films 518 (2010) e181–e182.
- [7] A. Khanna, R. Kumar, S.S. Bhatti, CuO-doped SnO<sub>2</sub> thin films as hydrogen sulphide gas sensor, Appl. Phys. Lett. 82 (2003) 4388–4390.
- [8] V.R. Katti, A.K. Debnath, K.P. Muthe, M. Kaur, A.K. Dua, S.C. Gadkari, S.K. Gupta, V.C. Sahni, Mechanism of drifts in H<sub>2</sub>S sensing properties of SnO<sub>2</sub>:CuO composite thin film sensors prepared by thermal evaporation, Sens. Actuators B 96 (2003) 245–252.

- [9] V. Kumar, S. Sen, K.P. Muthe, N.K. Gaur, S.K. Gupta, J.V. Yakhmi, Copper doped SnO<sub>2</sub> nanowires as highly sensitive H<sub>2</sub>S sensor, *Sens. Actuators B* 138 (2009) 587–590.
- [10] C.M. Ghimbeu, M. Lumbreiras, M. Siadat, R.C.V. Landschoot, J. Schoonman, Electrostatic sprayed SnO<sub>2</sub> and Cu-doped SnO<sub>2</sub> films for H<sub>2</sub>S detection, *Sens. Actuators B* 133 (2008) 694–698.
- [11] L.A. Patil, D.R. Patil, Heterocontact type CuO-modified SnO<sub>2</sub> sensor for the detection of a ppm level H<sub>2</sub>S gas at room temperature, *Sens. Actuators B* 120 (2006) 316–323.
- [12] J.M. Lee, B.U. Moon, C.H. Shim, B.C. Kim, M.B. Lee, D.D. Lee, J.H. Lee, H<sub>2</sub>S microgas sensor fabricated by thermal oxidation of Cu/Sn double layer, *Sens. Actuators B* 108 (2005) 84–88.
- [13] X. Kong, Y. Lee, High sensitivity of CuO modified SnO<sub>2</sub> nanoribbons to H<sub>2</sub>S at room temperature, *Sens. Actuators B* 105 (2005) 449–453.
- [14] M.S. Wagh, L.A. Patil, T. Seth, D.P. Amalnerkar, Surface cupricated SnO<sub>2</sub>–ZnO thick films as a H<sub>2</sub>S gas sensor, *Mater. Chem. Phys.* 84 (2004) 228–233.
- [15] A. Chowdhuri, S.K. Singh, K. Sreenivas, V. Gupta, Contribution of adsorbed oxygen and interfacial space charge for enhanced response of SnO<sub>2</sub> sensors having CuO catalyst for H<sub>2</sub>S gas, *Sens. Actuators B* 145 (2010) 155–166.
- [16] X. Zhou, Q. Cao, H. Huang, P. Yang, Y. Hu, Study on sensing mechanism of CuO–SnO<sub>2</sub> gas sensors, *Mater. Sci. Eng. B* 99 (2003) 44–47.
- [17] R.S. Niranjana, K.R. Patil, S.R. Sainkar, I.S. Mulla, High H<sub>2</sub>S-sensitive copper-doped tin oxide thin film, *Mater. Chem. Phys.* 80 (2003) 250–256.
- [18] R. Kumar, A. Khanna, P. Tripathi, R.V. Nandedkar, S.R. Potdar, S.M. Chaudhari, S.S. Bhatti, CuO–SnO<sub>2</sub> element as hydrogen sulphide gas sensor prepared by a sequential electron beam evaporation technique, *J. Phys. D: Appl. Phys.* 36 (2003) 2377–2381.
- [19] R.S. Niranjana, V.A. Chaudhary, I.S. Mulla, K. Vijayamohanana, A novel hydrogen sulphide room temperature sensor based on copper nanocluster functionalized tin oxide thin films, *Sens. Actuators B* 85 (2002) 26–32.
- [20] W. Yuanda, T. Maosong, H. Xiuli, Z. Yushu, D. Guorui, Thin film sensors of SnO<sub>2</sub>–CuO–SnO<sub>2</sub> sandwich structure to H<sub>2</sub>S, *Sens. Actuators B* 79 (2001) 187–191.
- [21] R.B. Vasiliev, M.N. Rummyantsev, N.V. Yakovlev, A.M. Gaskov, CuO/SnO<sub>2</sub> thin film heterostructures as chemical sensors to H<sub>2</sub>S, *Sens. Actuators B* 50 (1998) 186–193.
- [22] J. Tamaki, K. Shimanoe, Y. Yamada, Y. Yamamoto, N. Mirua, N. Yamazoe, Dilute hydrogen sulphide sensing properties of CuO–SnO<sub>2</sub> thin film prepared by low-pressure evaporation method, *Sens. Actuators B* 49 (1998) 121–125.
- [23] M.N. Rummyantseva, M. Labeau, J.P. Senateur, G. Delabouglise, M.N. Boulova, A.M. Gaskov, Influence of copper on sensor properties of tin dioxide films in H<sub>2</sub>S, *Mater. Sci. Eng. B* 41 (1996) 228–234.
- [24] E.R. Leite, M.I.B. Bernardi, E. Longo, J.A. Varela, C.A. Paskocimas, Enhanced electrical property of nanostructures Sb-doped SnO<sub>2</sub> thin film processed by soft chemical method, *Thin Solid Films* 449 (2004) 67–72.
- [25] A. Bouaine, N. Brihi, G. Schmerber, C. Ulhaq-Bouillet, S. Colis, A. Dinia, Structural, optical, and magnetic properties of Co-doped SnO<sub>2</sub> powders synthesized by the coprecipitation technique, *J. Phys. Chem. C* 111 (2007) 2924–2928.
- [26] S. Vijayalakshmi, S. Venkataraj, M. Subramanian, R. Jayavel, Physical properties of zinc doped tin oxide films prepared by spray pyrolysis technique, *J. Phys. D: Appl. Phys.* 41 (2008) 035505.
- [27] D. Chauhan, V.R. Satsangi, S. Dass, R. Shrivastava, Preparation and characterization of nanostructured CuO thin films for photoelectrochemical splitting of water, *Bull. Mater. Sci.* 29 (2006) 709–716.
- [28] M. Batzill, U. Diebold, The surface and materials science of tin oxide, *Prog. Surf. Sci.* 79 (2005) 47–154.

## Biographies

**Manish Verma** received his BSc (2005) and MSc (2007) degrees in Physics from University of Delhi, Delhi, India. Presently, he is a Senior Research Fellow (SRF) pursuing his PhD from Department of Physics and Astrophysics, University of Delhi. His research interest includes metal oxide thin film and nanoparticle based gas sensors.

**Vinay Gupta** received the BSc, MSc, and PhD degrees in physics in 1987, 1989, and 1995, respectively, from the University of Delhi, New Delhi, India. Presently, he is a professor in the Department of Physics and Astrophysics, University of Delhi. He is recipient of BOYSCAST fellow. He is a senior member of IEEE. His current research interests are in piezoelectric thin films and layered structures, semiconductor and surface acoustic wave (SAW) gas and bio-sensors, and nanostructure oxide materials for multifunctional application.